Robust Control of Two Link Rigid Manipulator

Pawan Singh Yadav and Narinder Singh

***Abstract*—Two Link Rigid Manipulator (TLRM) is highly unstable and non-linear system thus its stability is a matter of concern. This paper presents Lagrange-Euler method for deriving the dynamics of TLRM. The uncertain model is considered using LFT. Parametric uncertainty in moment of inertia and co-efficient of friction in the TLRM is considered and uncertainty in actuators. Two different robust control strategies, H_∞ and μ-synthesis are used and compared. Results show that μ-synthesis controller has superior robust performance of the proposed two robust control methods.**

***Index Terms*—H_∞ controller, linear fractional transformation (LFT), μ-synthesis controller, parametric uncertainty, robust control, two link rigid manipulator (TLRM).**

I. Introduction

Robot manipulators find wide application for dealing with radioactive or bio-hazardous materials or for use in inaccessible places. The existing manipulators shown to be inefficient if there is change in parameters of manipulator or of actuator then controlling the manipulator become a big problem therefore H_∞ and μ-synthesis design techniques are used to synthesize robot controllers. This spurred much research in this area. However an integrated approach in this regard has not been proposed so far.

A dynamic model for flexible manipulator using the Timoshenko beam theory is derived and μ-synthesis control design technique is used to synthesize the robot manipulator [1]. Uncertain system can also be analysed and controlled by the Adaptive control [2] and Robust control [3], [4] techniques. In order to control the robots a strategy which is derived using Lyapunov's direct method was proposed and the tracking problem of manipulators has been successfully solved but performance decreases when unknown loading masses or model disturbances are introduced [5]. A similar approach using Lyapunov synthesis method is used to minimize the force errors, further a robust adaptive tracking controller is proposed to guarantee the convergence of the trajectory tracking errors of multiple uncertain two-link manipulators [6].

Robots have received a considerable attention by different research groups. A dynamic model is designed for manipulating a two-rigid-link object applying two cooperative-arms and a PD controller with a disturbance observer to control the object lifting-up motion [7], although a disturbance observer minimizes the error but parametric uncertainty still needs to deal with.

Manuscript received June 21, 2014; revised September 15, 2014.
The authors are with the Department of Instrumentation and Control Engineering, Dr. B. R. Ambedkar National Institute of Technology, Jalandhar, India (e-mail: pawan.moonlight1301@gmail.com, singhn@nitj.ac.in).

Many research work for trajectory selection [8] and control of rigid-flexible two link [8], [9] and flexible manipulators have performed well but parameter uncertainty has not been considered so far as TLRM is concerned.

Robustness in control theory means a certain performance is guaranteed against external disturbances and noise [10]. In addition, it is noted that system parametric variation, which is caused by environmental changes or torn-and-worn factors, is an important class of uncertain systems with structured uncertainty [11]. A good approach for solving the problem of robust stability and stabilization is investigated for a class of continuous time uncertain system considering that uncertain system belongs to a polytopic convex set [11] and an electronics circuit is considered for application.

In all the previous research work, reference trajectory control and disturbance rejection of TLRM with parametric uncertainty has not been considered. In this paper, the reference trajectory, disturbance rejection and robust performance using H-infinity and μ-synthesis controllers has been compared. Both controllers show good robust stability.

II. Mathematical Modeling

A. Dynamic Modeling

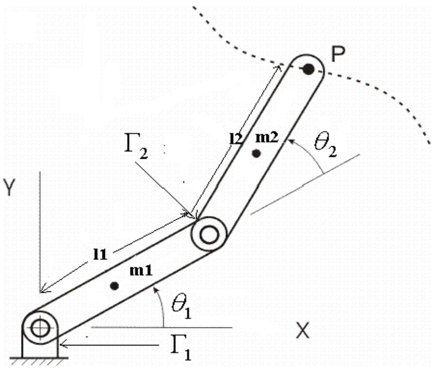

Fig. 1. Schematic diagram of two link rigid manipulator.

TABLE I: Parameters of Two-Link Rigid Manipulator

Symbol	Quantity	Typical value
M_1	Mass of Link 1	1 Kg
M_2	Mass of Link 2	1 Kg
L_1	Length of Link 1	0.3m
L_2	Length of Link 2	0.3m
τ_1, τ_2	Torque applied to joints	
θ_1, θ_2	Angular displacement of link1 from horizontal, Angular displacement of link2 with respect to link1	

m = meter, kg = kilogram

It consists of two revolute joints to provide angular motion between the links. To move the link, controlling torque is applied by the actuator at the manipulator joint. The dynamic equations of the system are derived using Lagrange Euler Formulation. TLRM is shown in Fig. 1. The parameters for TLRM are given in Table I.

The serial link modeled by systematically using physical laws of Lagrangian mechanics to develop the manipulator Equations of Motion (EOM). Lagrangian L is defined as the difference between the total kinetic energy K and the total potential energy P of a mechanical system.

$$L = K - P \tag{1}$$

The dynamic model based on Lagrange Euler formulation is obtained from the Lagrangian, as a set of equations,

$$\frac{d}{dt}\left(\frac{\partial L}{\partial q_i}\right) - \frac{\partial L}{\partial q_i} = \tau_i \quad \text{For } i = 1,\ 2, ...,\ n \tag{2}$$

Considering the co-efficient of friction C, the generalized Lagrange Euler equation can be modified as:

$$\tau_1 = M_{11}\ddot{\theta}_1 + M_{12}\ddot{\theta}_2 + H_1 + G_1 + C_1\dot{\theta}_1 - C_2(\dot{\theta}_2 - \dot{\theta}_1) \tag{3}$$

$$\tau_2 = M_{21}\ddot{\theta}_1 + M_{22}\ddot{\theta}_2 + H_2 + G_2 + C_2(\dot{\theta}_2 - \dot{\theta}_1) \tag{4}$$

where M_{ii}=effective inertia, M_{ij}=effective coupling inertia, H_i & G_i=centrifugal and coriolis acceleration forces. Since both joint are revolute, the generalized torques τ_1 and τ_2 represent the actual join torques and the following equation represents EOM of the Two-link planar manipulator.

$$\begin{bmatrix}\tau_1\\ \tau_2\end{bmatrix} = \begin{bmatrix}M_{11} & M_{12}\\ M_{21} & M_{22}\end{bmatrix}\begin{bmatrix}\ddot{\theta}_1\\ \ddot{\theta}_2\end{bmatrix} + \begin{bmatrix}-2H\dot{\theta}_2 + C_1 + C_2 & -H\dot{\theta}_2 - C_2\\ H\dot{\theta}_1 - C_2 & C_2\end{bmatrix}\begin{bmatrix}\dot{\theta}_1\\ \dot{\theta}_2\end{bmatrix} + \begin{bmatrix}G_1\\ G_2\end{bmatrix} \tag{5}$$

$$M_{11} = \left[\left(\frac{1}{3}m_1 + m_2\right)L_1^{\,2} + \frac{1}{3}m_2 L_2^{\,2} + m_2 L_2 L_2 c_2\right]$$

$$M_{12} = M_{21} = m_2\left[\frac{1}{3}L_2^{\,2} + \frac{1}{2}L_1 L_2 c_2\right]$$

$$M_{22} = \frac{1}{3}m_2 L_2^{\,2};\ H_1 = -m_2 L_1 L_2 s_2 \dot{\theta}_1\dot{\theta}_2 - \frac{1}{2}m_2 L_1 L_2 s_2 \dot{\theta}_2^{\,2}$$

$$H_2 = \frac{1}{2}m_2 L_1 L_2 s_2 \dot{\theta}_1^{\,2}$$

$$G_1 = \left(\frac{1}{2}m_1 + m_2\right)g L_1 c_1 + \frac{1}{2}m_2 g L_2 c_{12}$$

$$G_2 = \frac{1}{2}m_2 g L_2 c_{12}$$

B. LFT Modeling

Considering parametric uncertainty in moment of inertia and co-efficient of friction of the two links. The system block diagram with uncertain parameters is shown in the Fig. 2.

$$I_i = \overline{I_i}(1 + \delta_i P_i) \tag{6}$$

$$C_1 = \overline{C_{I_i}}(1 + \delta_{C_i} S_i) \tag{7}$$

where $\overline{I_i}$ & $\overline{C_{I_i}}$ are the nominal values of the corresponding moment of inertia and co-efficient of friction respectively, P_i = 0.10 and S_i=0.20 is the maximum relative uncertainty in each of these cases and $(-1 \le \delta_i, \delta_{C_i} \le +1)$; i = 1, 2, 3….

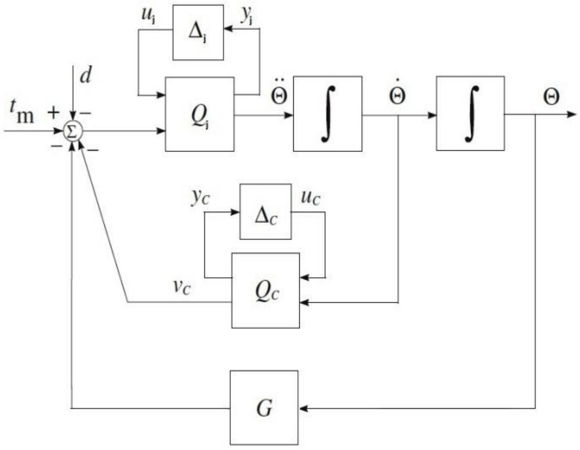

Fig. 2. System block diagram with uncertain parameters.

Now linearise the model and let us assume the State Space Parameters:

$$x_1 = \theta_1;\quad x_2 = \theta_2;\quad x_3 = \dot{\theta}_1;\quad x_4 = \dot{\theta}_2;\quad y = \theta$$

The State equation and Output equation are as follows:

$$\begin{bmatrix}\dot{x}_1\\ \dot{x}_2\\ \dot{x}_3\\ \dot{x}_4\end{bmatrix} = \begin{bmatrix}0 & 0 & 1 & 0\\ 0 & 0 & 0 & 1\\ -112.11 & 70.07 & -2.79 & 1.54\\ 280.28 & -224.22 & 7.75 & -4.64\end{bmatrix}\begin{bmatrix}x_1\\ x_2\\ x_3\\ x_4\end{bmatrix} +$$

$$\begin{bmatrix}0 & 0 & 0 & 0 & 0 & 0 & 0 & 0\\ 0 & 0 & 0 & 0 & 0 & 0 & 0 & 0\\ -0.01 & 0.021 & -0.24 & 0.30 & -19.04 & 47.61 & 19.04 & -47.61\\ 0.02 & -0.05 & 0.62 & -0.92 & 47.61 & -152.38 & -47.61 & 152.38\end{bmatrix}\begin{bmatrix}u_j|_{2\times1}\\ u_c|_{2\times1}\\ d|_{2\times1}\\ \tau|_{2\times1}\end{bmatrix}$$

$$\begin{bmatrix}y_j\\ y_c\\ y\end{bmatrix} = \begin{bmatrix}-112.11 & 70.07 & -2.79 & 1.54\\ 280.28 & -224.22 & 7.75 & -4.64\\ 0 & 0 & 1 & 0\\ 0 & 0 & -1 & 1\\ 1 & 0 & 0 & 0\\ 0 & 1 & 0 & 0\end{bmatrix}\begin{bmatrix}x_1\\ x_2\\ x_3\\ x_4\end{bmatrix} +$$

$$\begin{bmatrix}-0.014 & 0.02 & -0.24 & 0.30 & -19.04 & 47.61 & 19.04 & -47.61\\ 0.02 & -0.05 & 0.62 & -0.92 & 47.61 & -152.38 & -47.61 & 152.38\\ 0 & 0 & 0 & 0 & 0 & 0 & 0 & 0\\ 0 & 0 & 0 & 0 & 0 & 0 & 0 & 0\\ 0 & 0 & 0 & 0 & 0 & 0 & 0 & 0\\ 0 & 0 & 0 & 0 & 0 & 0 & 0 & 0\end{bmatrix}\begin{bmatrix}u_j|_{2\times1}\\ u_c|_{2\times1}\\ d|_{2\times1}\\ \tau|_{2\times1}\end{bmatrix}$$

The uncertain behavior of the whole system can be described by an upper LFT representation as shown in Fig. 3.

Thus the open-loop manipulator model is an eight-input and eight-output system.

$$\begin{bmatrix}y_j\\ y_c\\ y\end{bmatrix} = G_{man}\begin{bmatrix}u_j\\ u_c\\ d\\ \tau\end{bmatrix}$$

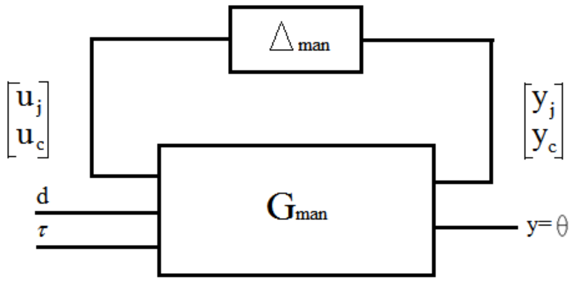

Fig. 3. LFT representation of perturbed two-link rigid manipulator.

$$G_{man}=\begin{bmatrix}[A]_{4\times4} & [B_1]_{4\times4} & [B_2]_{4\times4}\\ [C_1]_{4\times4} & [D_{11}]_{4\times4} & [D_{12}]_{4\times4}\\ [C_2]_{2\times4} & [D_{21}]_{2\times4} & [D_{22}]_{2\times4}\end{bmatrix};\ \Delta_{man}=\begin{bmatrix}\Delta_j & 0\\ 0 & \Delta_c\end{bmatrix}$$

C. Open Loop Interconnected System

The structure of the open-loop system is shown in Fig. 4. The actuators are taken as first order phase-lag model and approximated by input multiplicative uncertainty. The variables pertin and pertout (input and output to G_{man}) have four elements, and the variables control, dist, e_p , e_u and y_c have two element each.

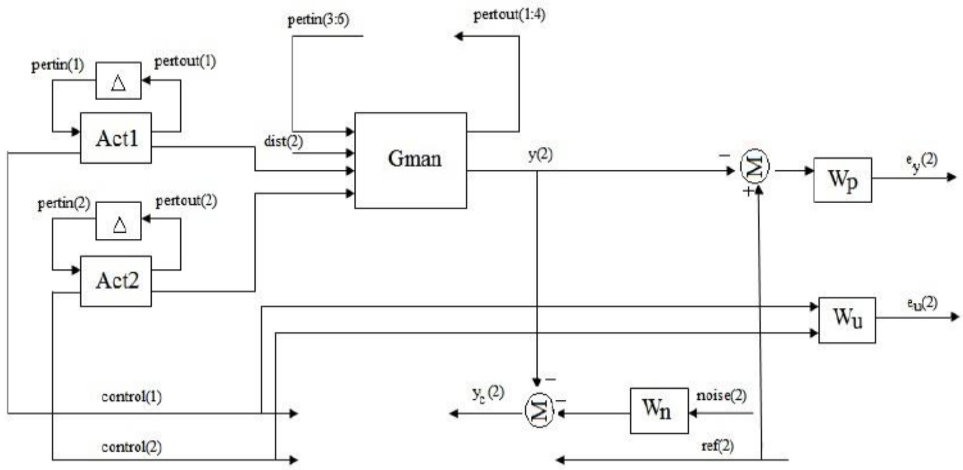

Fig. 4. Open loop interconnection of two link rigid manipulator.

The parameters in Fig. 4 are as follows:

$$W_P=\begin{bmatrix}w_{p_1}(s) & 0\\ 0 & w_{p_2}(s)\end{bmatrix};w_{p_1}=w_{p_2}=\frac{s^2+2s+3}{1.01s^2+3s+0.005}$$

$$W_U=\begin{bmatrix}w_u(s) & 0\\ 0 & w_u(s)\end{bmatrix};w_u=10^{-6}$$

$$W_n=\begin{bmatrix}w_n(s) & 0\\ 0 & w_n(s)\end{bmatrix};w_n=2\times10^{-5}\frac{10s+1}{0.1s+1}$$

The transfer function matrix W_p is performance weight and W_u is control weight. The optimized weighting functions are chosen to achieve the best performance of TLRM. W_n is weighing function for shaping filter on the measurement noise.

III. Robust Controller Design

A. H_∞ Controller

H_∞ (sub) optimal control law for system interconnection structure is given by the block diagram in Fig. 5. The H_∞ optimal control minimizes the $\|.\|_\infty$norm of $F_L(P, K)$ over the stabilizing controller transfer matrix K, where P is the transfer function matrix of the augmented system. In the given case $F_L(P, K)$ is the nominal closed loop system transfer matrix from the references, disturbances and noises (the signals r, d and η) to the weighted outputs e_y and e_u. The range of γ is selected between 1.0 and 10.0 with a tolerance 0.001. The closed loop system achieved γ equal to 0.0005.

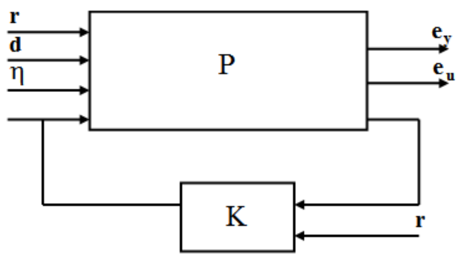

Fig. 5. Block diagram of H_∞ design.

B. μ-Synthesis Controller

The block structure Δ_P of uncertainties is defined as

$$\Delta_P:=\left\{\begin{bmatrix}\Delta_1 & 0\\ 0 & \Delta_2\end{bmatrix}:\Delta_1\in R^{6\times6},\Delta_2\in C^{6\times4}\right\}$$

The first block of the matrix Δ_P, the uncertainty block Δ_1 corresponds to the parametric uncertainties modeled in the TLRM. The second block, Δ_2 is a fictitious uncertainty block, introduced to include the performance objectives in the framework of the μ-approach.

To meet the design objectives a stabilizing controller K is to be found such that, at each frequency $\omega\in[0,\infty]$, the structured singular value μ satisfies the condition

$$\mu_{\Delta_P}[F_L(P,K)(j\omega)]<1$$

The progress of the D-K iteration is shown in Table II. It can be seen from the table that after the third iteration the maximum value of μ is equal to 0.996, which indicates that the robust performance has been achieved. The final controller obtained is of 26th order.

TABLE II: D-K ITERATION RESULT OF μ-SYNTHESIS CONTROLLER

Iteration	Controller order	Maximum value of μ
1	14	163.261
2	36	2.101
3	26	0.991

IV. SIMULATION AND RESULTS

Two link rigid manipulatorb(TLRM) with the controllers are designed in MATLAB and their transient responses and disturbance rejection are shown in Fig. 5 and Fig. 7.

A. H_∞ Controller

Fig. 6(a) and Fig. 6(b) show the closed-loop transient response of H_∞ controller. The transient response is fast having settling time for θ_1 and θ_2 approximately equals 5.3 sec and 5.2 sec respectively with small overshoots of output variables. Fig. 7(a) and Fig. 7(b) show Disturbance rejection of H_∞ controller.

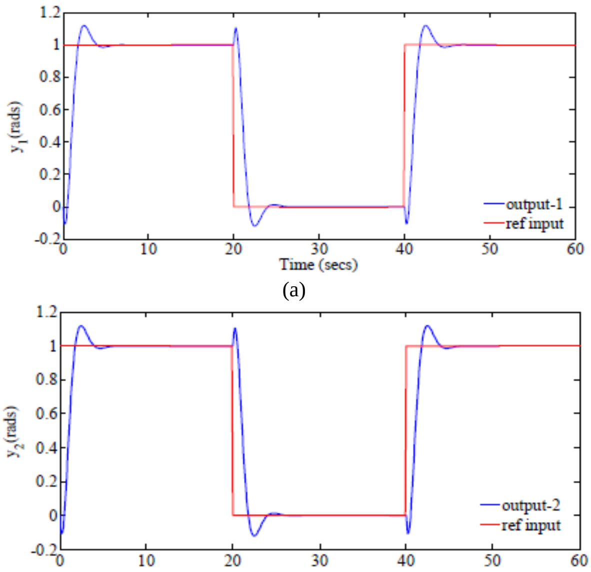

Fig. 6. H∞ controller (a). Transient response ($\theta 1$) (b). Transient response ($\theta 2$).

The closed-loop system achieves robust stability if the closed loop system is internally stable for all of the possible plant models:

$$\mathrm{KG_{nom}}\left(I+KG_{nom}{}^{-1}\right)_\infty < 1$$

The closed-loop system achieves robust performance if the closed loop system already achieved robust stability for all of the possible plants models and performance objective is also satisfied:

$$W_p\left(I+GK\right)^{-1}{}_\infty < 1$$

Fig. 8 clearly shows the Robust stability satisfying the criteria for stability since the maximum value of μ is 0.2821. Fig. 9 clearly shows that the closed-loop system does not achieve robust performance because the maximum value of μ is 1.0034. Hence it is concluded that the designed H_∞ controller leads to good transient response and system stability but at the same time does not ensure good robust performance. Hence, there is need for another controller which improves the transient response and ensures the robust stability as well as robust performance.

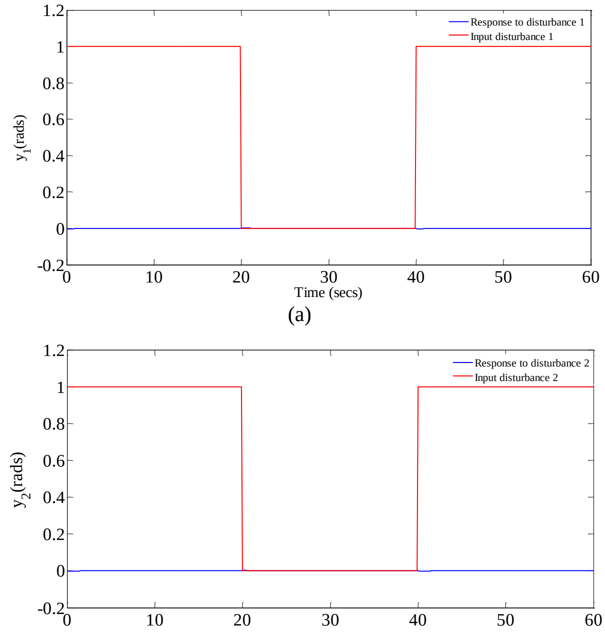

Fig. 7. H_∞ controller (a). Disturbance rejection-1 (b). Disturbance rejection-2.

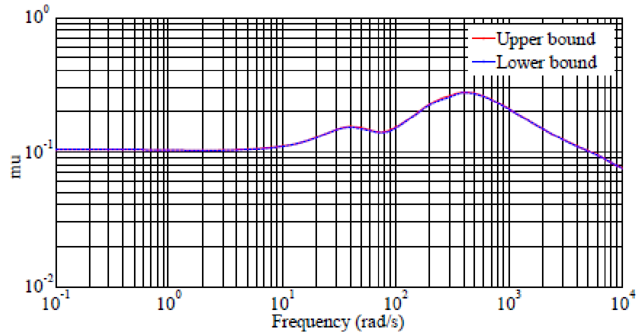

Fig. 8. Robust stability of H_∞ controller.

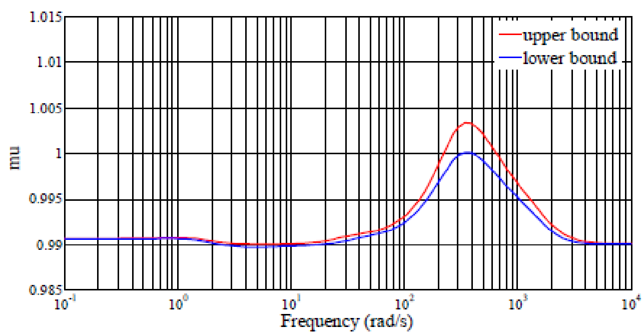

Fig. 9. Robust performance of H_∞ controller.

B. μ-Synthesis Controller

Fig. 10 and Fig. 11 show the transient response and disturbance rejection of the μ-synthesis controller. The transient response is very fast having settling time for θ_1 and θ_2 approximately equals 4.4 sec and 4.8 sec respectively. Moreover peak overshoot is also quite small as compared to H-infinity controller.

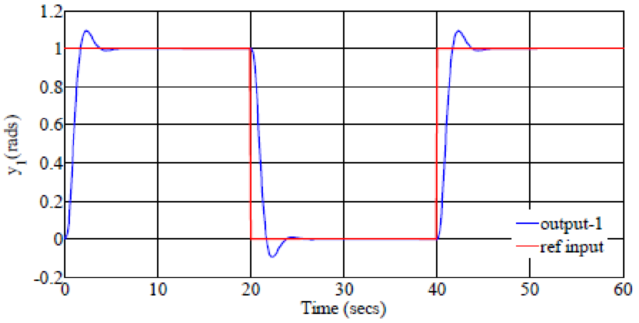

(a)

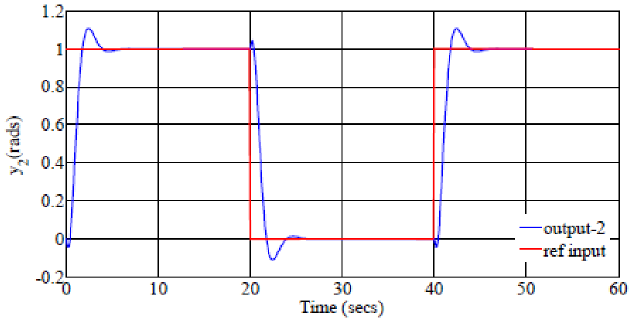

(b)

Fig. 10. μ-synthesis controller (a) Transient response (1); (b) Transient response (2).

Thus, overall transient response of the system has been improved. Moreover there is no steady state error in the system.

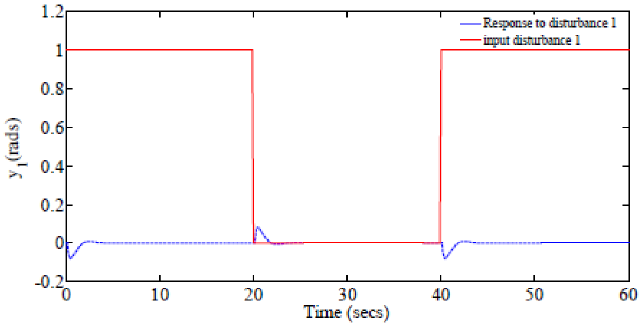

(a)

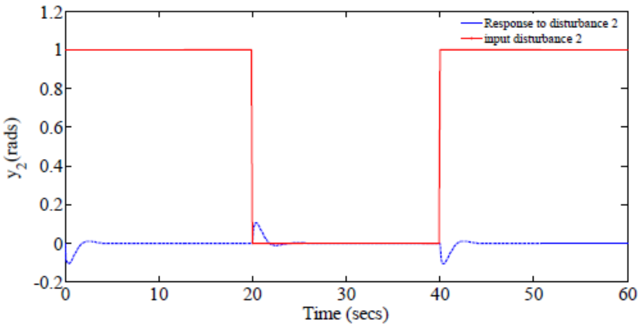

(b)

Fig. 11. μ-synthesis controller (a) Disturbance rejection-1; (b) Disturbance rejection-2.

Fig. 12(a) shows the robust stability and robust performance of μ-synthesis controller. Robust stability having maximum value of μ equals 0.1900 thus satisfying the criteria for stability. Fig. 12(b) shows the maximum value of μ in is 0.9936 which is less than 1 thus ensures good robust performance.

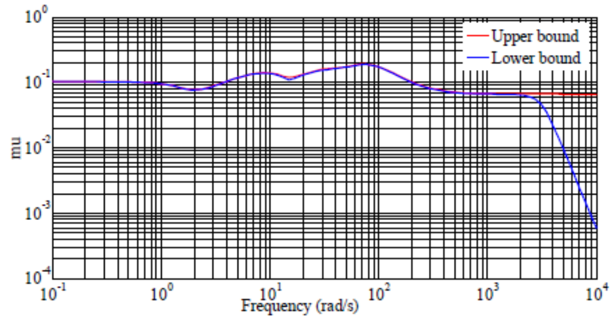

(a)

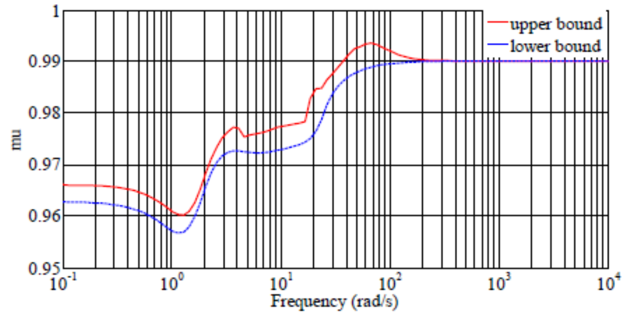

(b)

Fig. 12. μ-synthesis controller (a) Robust stability; (b) Robust performance.

V. Conclusion

In this paper H-infinity controller and μ-synthesis controllers are successfully designed using MATLAB for two link rigid manipulator (TLRM). Based on the results obtained, both controllers are capable of stabilizing the manipulator very effectively but the transient response in case of H_∞ controller is having a slight longer settling time which is improved when using μ-synthesis controller, but this comes on the cost of disturbance rejection which is slightly poor in μ-synthesis controller. However, the graph of robust performance ensures that μ-synthesis controller has superior performance as compared to H-infinity controller.

References

[1] M. Karkoub and K. Tamma, "Modelling and mu-synthesis control of flexible manipulators," *Computers and Structures*, vol. 79, pp. 543-551, May 2000.

[2] F. Pourboghra and P. Karlsson, "Adaptive control of dynamic mobile robots with non-holonomic constraints," *Comput. Elect. Eng.*, vol. 28, no. 3, pp. 241-253, 2002.

[3] G. Lee and F. Cheng, "Robust control of manipulators using the computed torque plus H1 compensation method," *IEEE Proc. Cont. Theory Appl.*, vol. 143, pp. 64-72, 1996.

[4] F. Lin and R. D. Brandt, "An optimal control approach to robust control of robot manipulators," presented at IEEE International Conference on Control Applications, Dearborn, USA, September 15-18, 1996.

[5] S. Torres, J. A. Me ́ndeza, L. Acostaa, and V. M. Becerra, "On improving the performance in robust controllers for robot manipulators with parametric disturbances," *Control Engineering Practice*, vol. 15, pp. 557-566, 2007.

[6] H. Dou and S. Wang, "Robust adaptive motion/force control for motion synchronization of multiple uncertain two-link manipulators," *International Journal of Mechanism and Machine Theory*, vol. 67, pp. 77-93, 2013.

[7] Z. Zyada, Y. Hayakawa, and S. Hosoe, "Model-based control for nonprehensile manipulation of a two-rigid-link object by two cooperative arms," presented at IEEE Conference on Robotic and Biomimetics, Tianjin (China), December 14-18, 2010.

[8] A. A. Ata, "Trajectory selection for a rigid/flexible manipulator," presented at IEEE International Conference on Industrial Technology (ICIT), Athens, March 19-21, 2012.

[9] S. Choura, "Control of a two-link rigid/flexible manipulator with a moving payload mass," *Journal of Sound and Vibration*, vol. 243, no. 5, pp. 883-897, 2001.

[10] P. Liu, "Delay-dependent robust stability analysis for recurrent neural networks with time-varying delay," *Int. J. Innov. Comput., Inf. Control*, vol. 9, no. 8, pp. 3341-3355, Aug. 2013.

[11] X. Zhao, L. Zhang, and P. Shi, "Robust control of continuous-time systems with state-dependent uncertainties and its application to electronic circuits," *IEEE Transaction on Industrial Electronics*, vol. 61, no. 8, pp. 4161-4170, Aug. 2013.

Pawan Singh Yadav was born at Allahabad on 13th January 1991. He obtained his bachelor's degree from the State University (UPTU) in 2012. He is currently a M.Tech scholar pursuing from Dr. B. R. Ambedkar NIT, Jalandhar, Punjab. His research is focused on robust stability and robust performance of rigid manipulators.

Narinder Singh Bhangal has done his B.Tech in electrical Engg. from Punjab University, Chandigarh, India in 1984 and did his M.Tech in control systems from Punjab Agricultural University, Ludhiana, Punjab, India. Currently he is working as a head, in the Dept of Electrical Engg. at National Institute of Technology, Jalandhar, Punjab. His area of research is optimal control, fuzzy, neuro-fuzzy control and currently doing Ph.D in robust control of flexible manipulators.